Supporting Information

Investigation of Hypoxia-induced Myocardial Injury Dynamics in a Tissue Interface Mimicking Microfluidic Device

Li Ren,[†,§] Wenming Liu,[†,§] Yaolei Wang,[†,§] Jian-Chun Wang,[†] Qin Tu,[†] Juan Xu,[†] Rui Liu,[†]

Shao-Fei Shen,[†] and Jinyi Wang[†,‡]*

[†]Colleges of Veterinary Medicine and Science, and [‡]Shaanxi Key Laboratory of Molecular Biology for Agriculture, Northwest A&F University, Yangling, Shaanxi 712100, People's Republic of China

Abstract

Supporting Information includes all additional information as noted in the manuscript.

Design of the Micropillar Structure in the Microfluidic Device. According to our previous study[1] and other microenvironment-controlled cell culture microfluidic devices,[2,3] two types of micropillar structures were first designed in the microfluidic devices, type 1: 20 μm in diameter, 4 μm in space, 5 μm in height; type 2: 20 μm in diameter, 6 μm in space, 5 μm in height. On-chip mass transportation and distribution were then evaluated to optimize the micropillar structure for the next study. The channels and the chamber in the device were treated with collagen-I (200 μg/mL, 2 h) similar to the microfluidic cell culture pre-treatment to improve their hydrophilic condition and the biologically relevant microenvironment. Fluorescein (100 μM fluorescein in $NaHCO_3$ buffer, pH 8.3) was used in the present study as a model cue. It was introduced from one inlet into the side channel using a syringe pump (LSP01-1A, Longer Pump) to characterize visually the solute distribution in the device. Fresh $NaHCO_3$ buffer was simultaneously injected into the other side channel at the same flow rates (0.5 μL/min or 1 μL/min). Each experiment was repeated at least three times. For the type 1 of the micropillar structure, both the increasing fluorescein concentration and the broadening gradient in the cell culture chamber were positively related to the increasing flow. In addition, fluorescein zone and non-fluorescein zone coexisted in the cell culture chamber (Figure S1A). Compared with type 1, a higher and broader concentration gradient occurred in the type 2 device. The fluorescein occupied the entire cell chamber and the influence of increasing flow on the fluorescein distribution was not significant (Figure S1B). Based on the biological truth that the volume of blood flow in capillaries relates to the degree of local tissue perfusion,[4] the type 1 of micropillar structure was used in this study for facilitating mimicking physiological fluidic microenvironment and hypoperfusion/hypoxia condition during myocardial infarction.

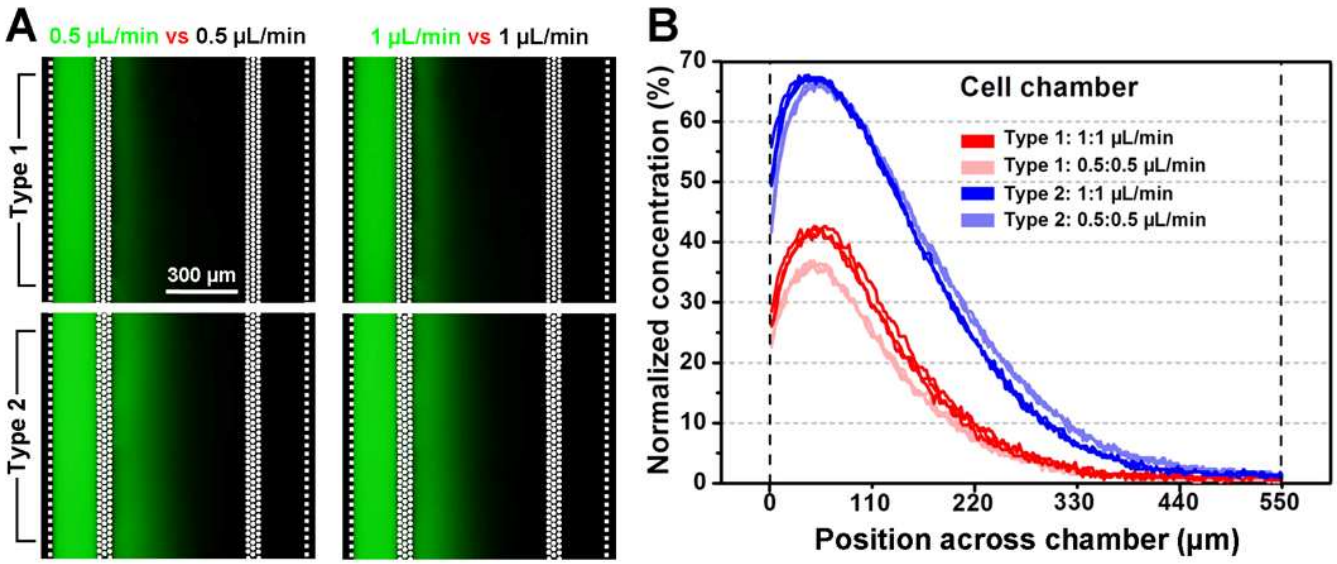

Figure S1. Mass distribution in microfluidic devices with different types of micropillar structures (type 1 and type 2) using fluorescence visualization at 0.5 µL/min and 1 µL/min at the side channels. (A) Observable mass distribution based on different types of micropillar structures. (B) Quantitative concentration distribution. The results show that type 2 micropillars can result in a higher and broader concentration gradient than type 1 micropillars at the same flow rate. Meanwhile, the gradient was not significantly changed at different flow rates in the device with type 2 micropillars, which suggests less flow-induced influence to concentration gradient formation. On the other hand, type 1 micropillars can realize a positively flow-influenced change of concentration gradient.

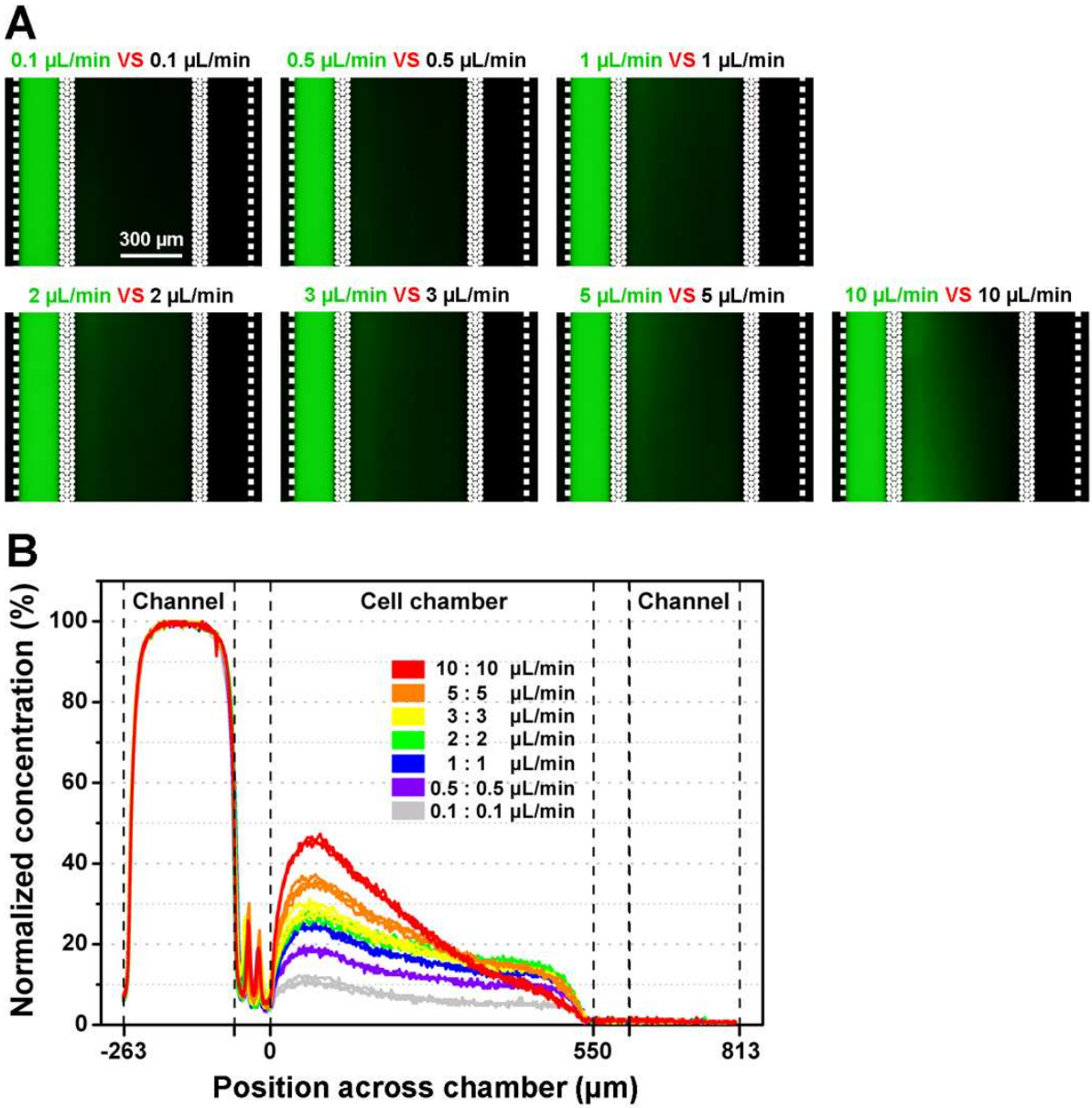

Figure S2. Mass distribution at the closed state (i.e., the central inlet and outlet were blocked) in the device using fluorescence visualization and a series of biologically relevant flows (0.1 μL/min to 10 μL/min in the two side channels). (A) Observable mass distribution at different flow rates. (B) Quantitative concentration distribution at different flow rates. The concentration of the solute in the chamber is lower than that at the open condition (Figures 2A and 2B in the text).

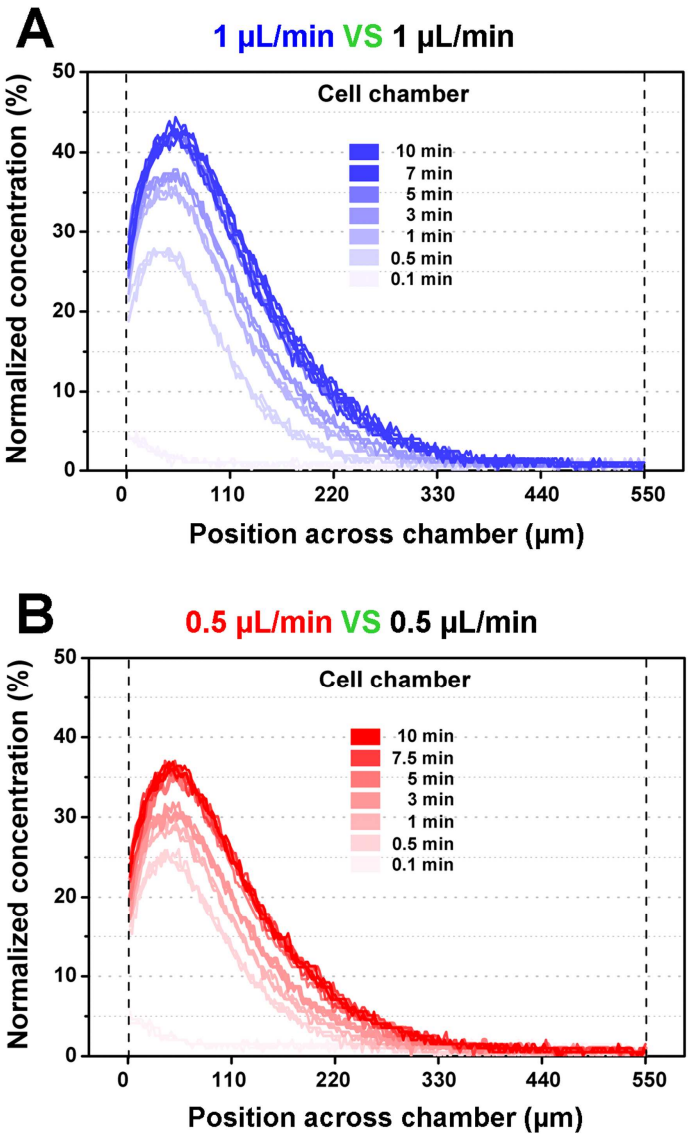

Figure S3. Temporal changes in mass distribution using fluorescence visualization in the open condition at 1 µL/min (A) and 0.5 µL/min (B).

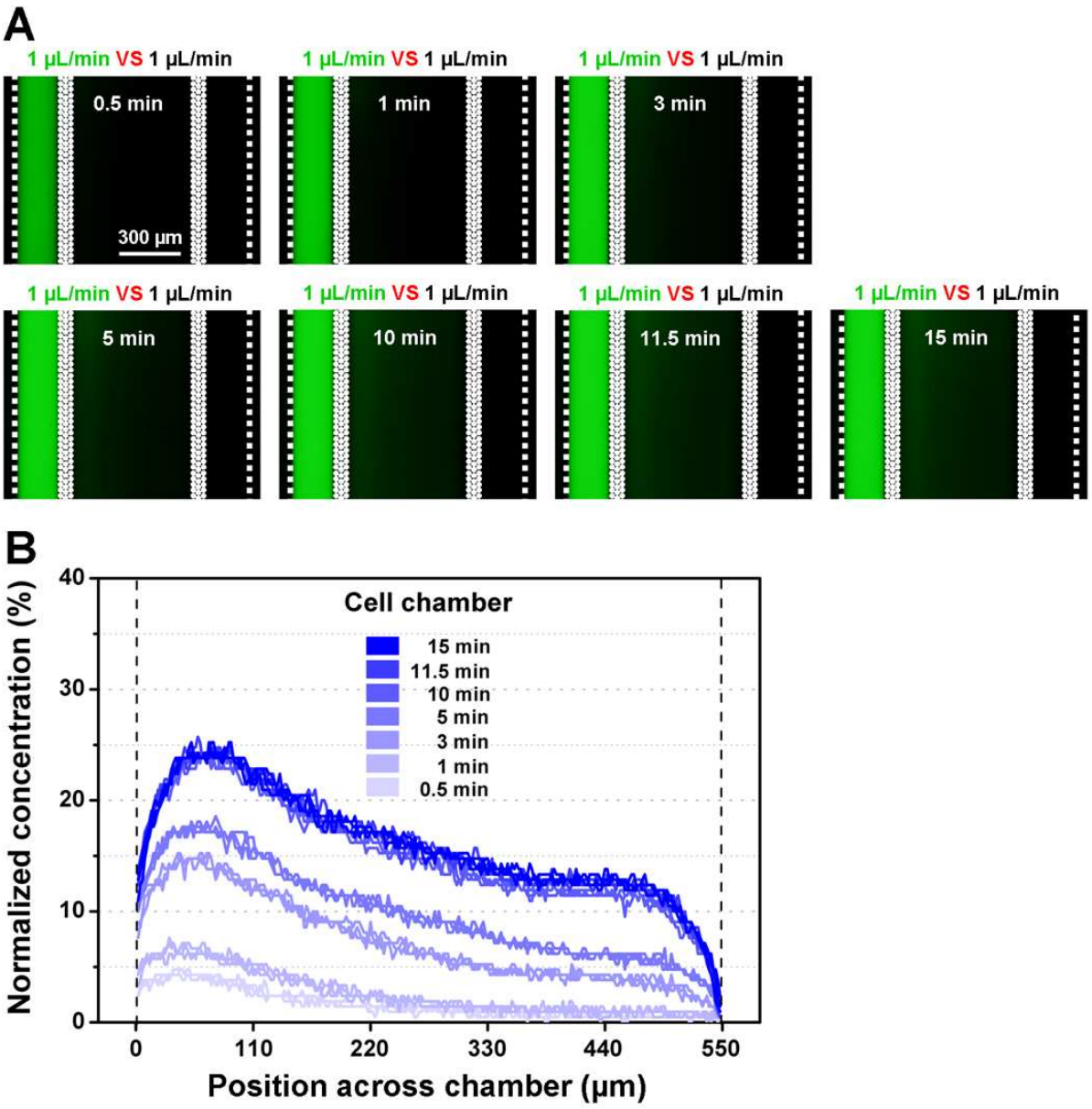

Figure S4. Mass distribution at the closed state (i.e., the central inlet and outlet were blocked) in the device using fluorescence visualization at 1 μL/min in the side channels. (A) Observable mass distribution at different perfusion times. (B) Quantitative concentration distribution. The solute transportation into the chamber is slower than that in the open condition and at the same flow rate [Figure S3(A)].

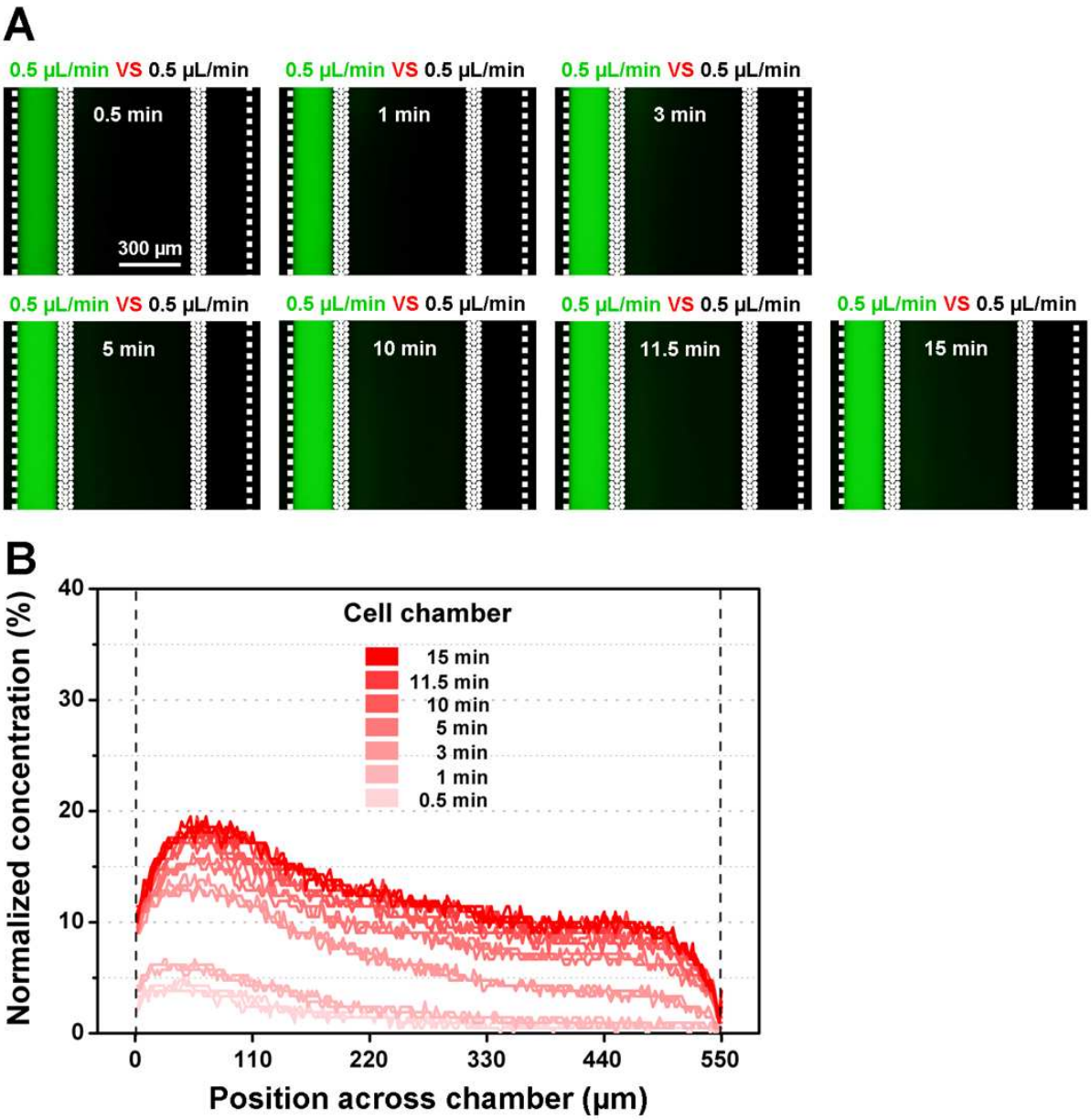

Figure S5. Mass distribution at the closed state (i.e., the central inlet and outlet were blocked) in the device using fluorescence visualization at 0.5 μL/min in the side channels. (A) Observable mass distribution at different perfusion times. (B) Quantitative concentration distribution. The results suggest that the solute transportation into the chamber is slower than that in the open condition and at the same flow rate [Figure S3(B)].

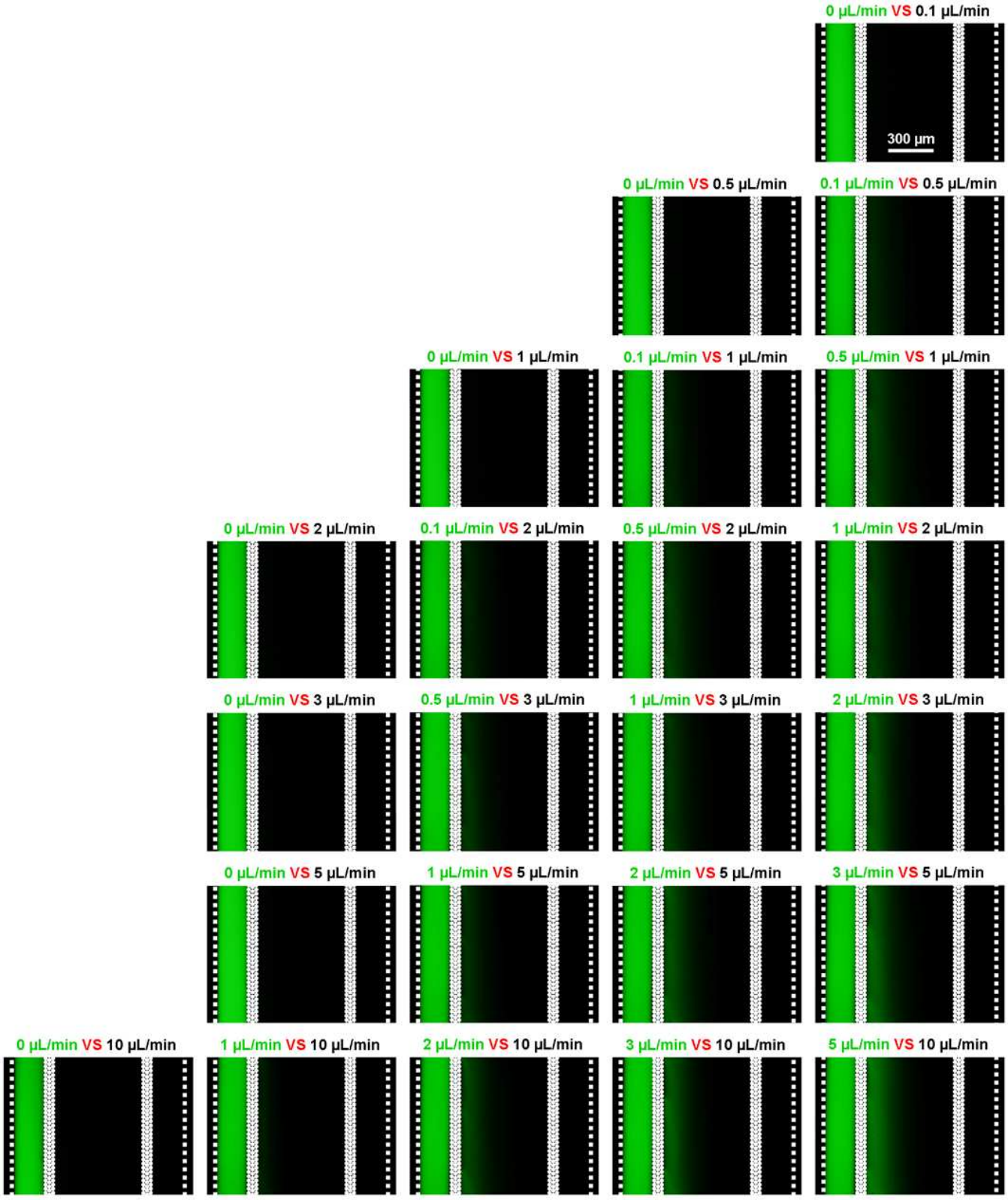

Figure S6. Fluorescence-assisted mass transportation in the open condition and at different flow rates between the two side channels.

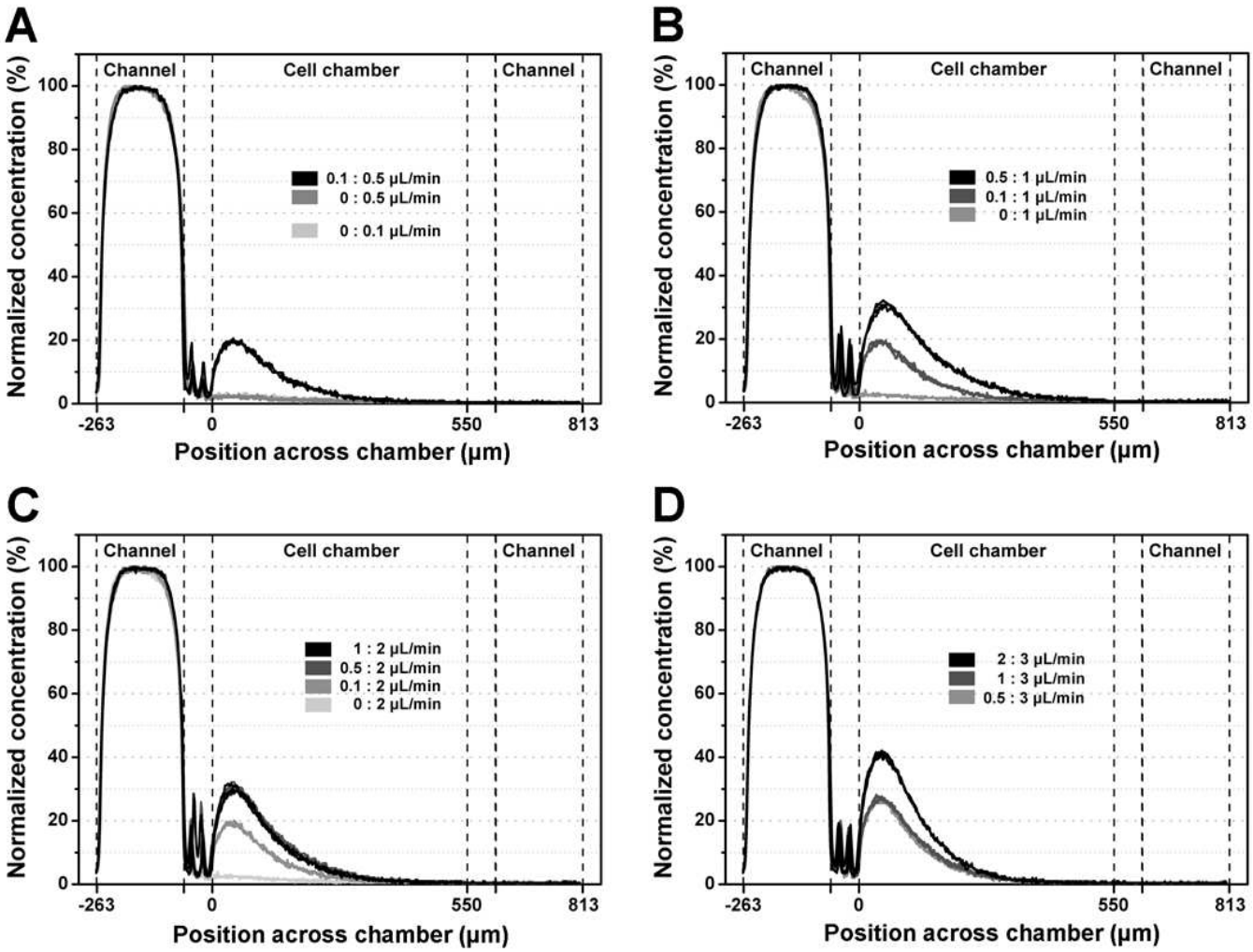

Figure S7. Quantitative analysis of mass transportation and distribution in the open condition and at different flow rates between the two side channels. The mass distribution in the chamber returned to the P channel (the left channel), and the flow rate in the P channel decreased.

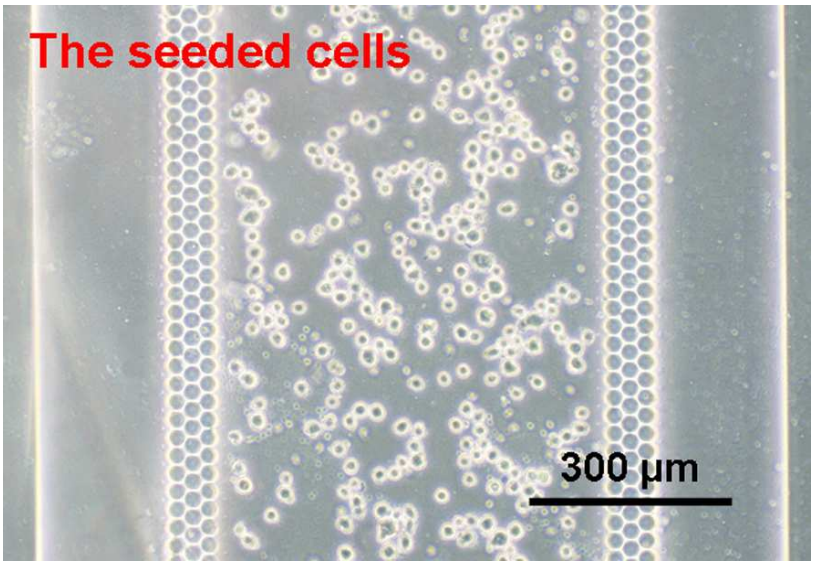

Figure S8. Optical image of the seeded myocardium H9c2 cells in the cell culture chamber.

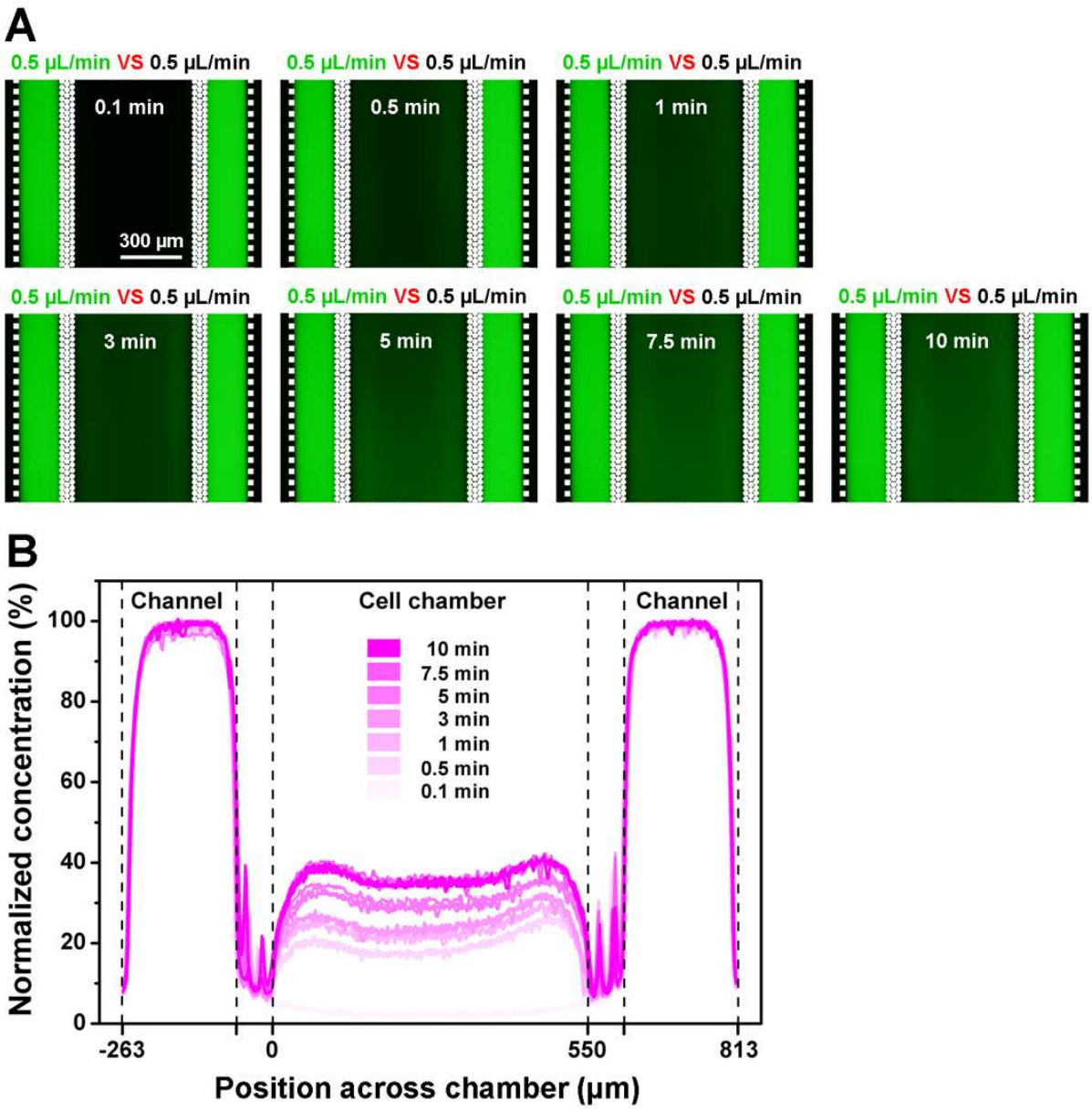

Figure S9. Fluorescence-aided nutrient supply evaluation of myocardial cell cultivation. (A) Fluorescent mass distribution at different perfusion times. (B) Quantitative analysis of concentration distribution. The solute concentration in the chamber is relatively uniform and is close to 40% compared with that in the side channel.

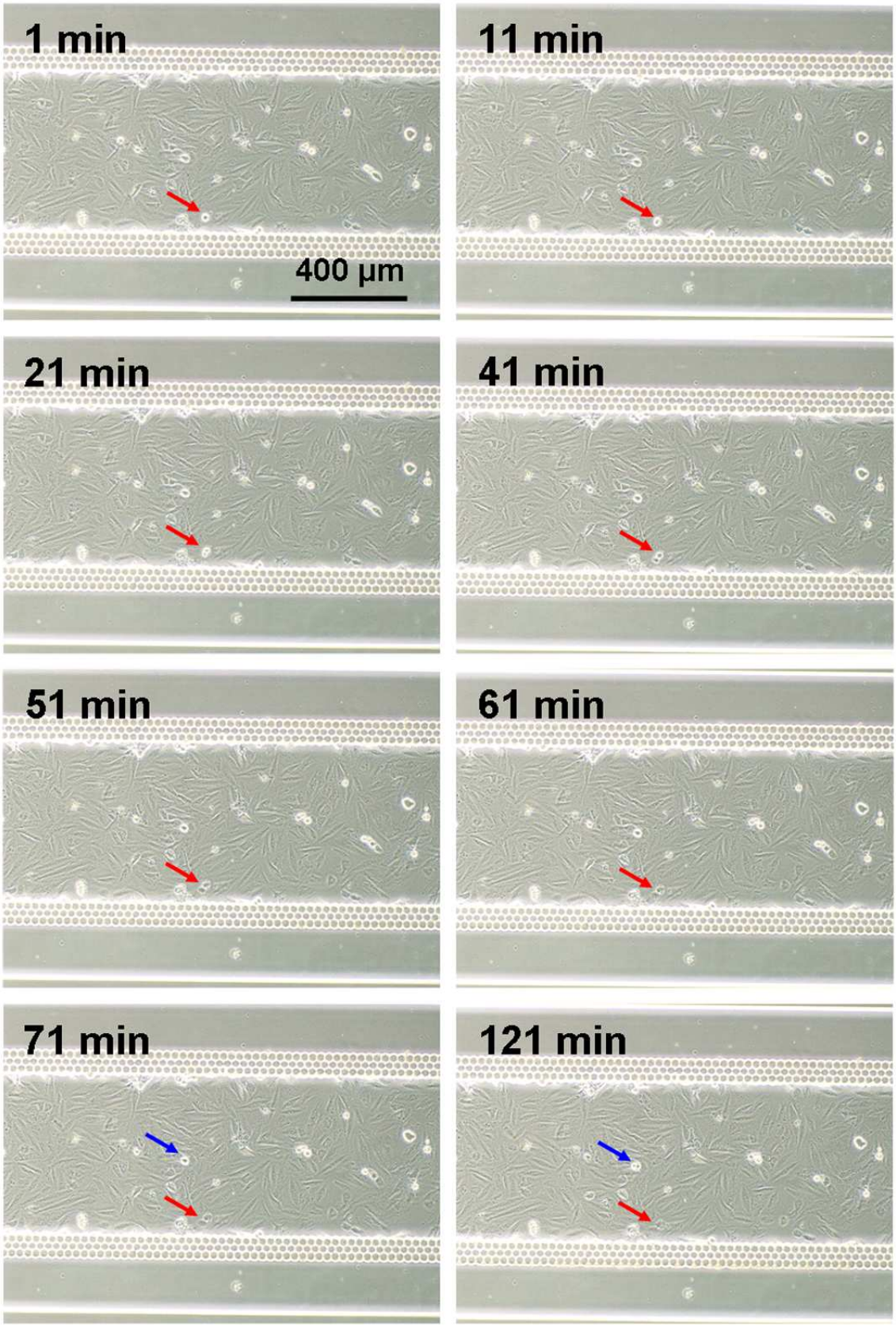

Figure S10. Growth and proliferation (red and blue arrows) of myocardial cells in the chamber.

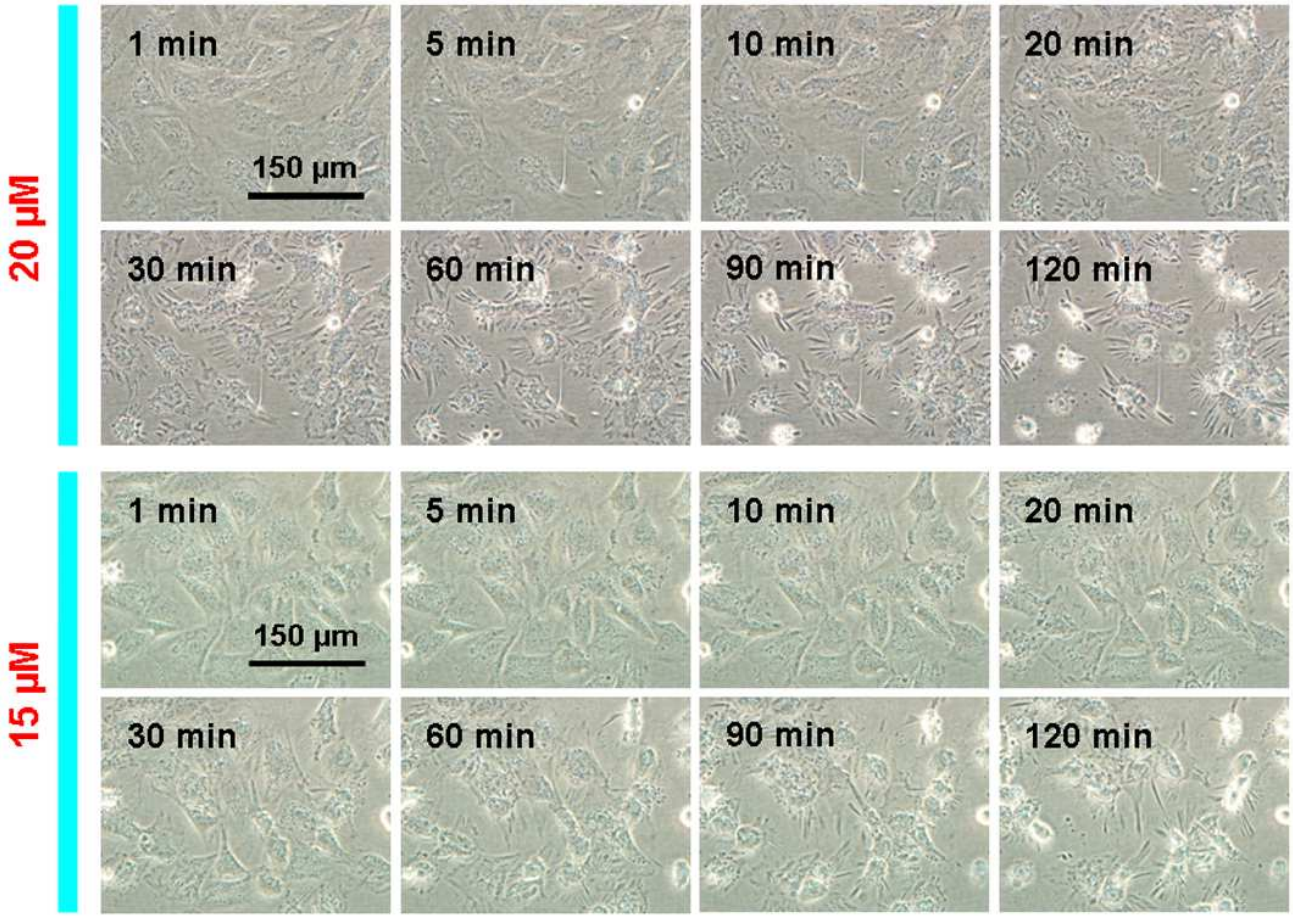

Figure S11. Morphological changes in the myocardial cells during FCCP hypoxia treatment at a concentration of 15 μM and 20 μM using the conventional plate-based culture method.

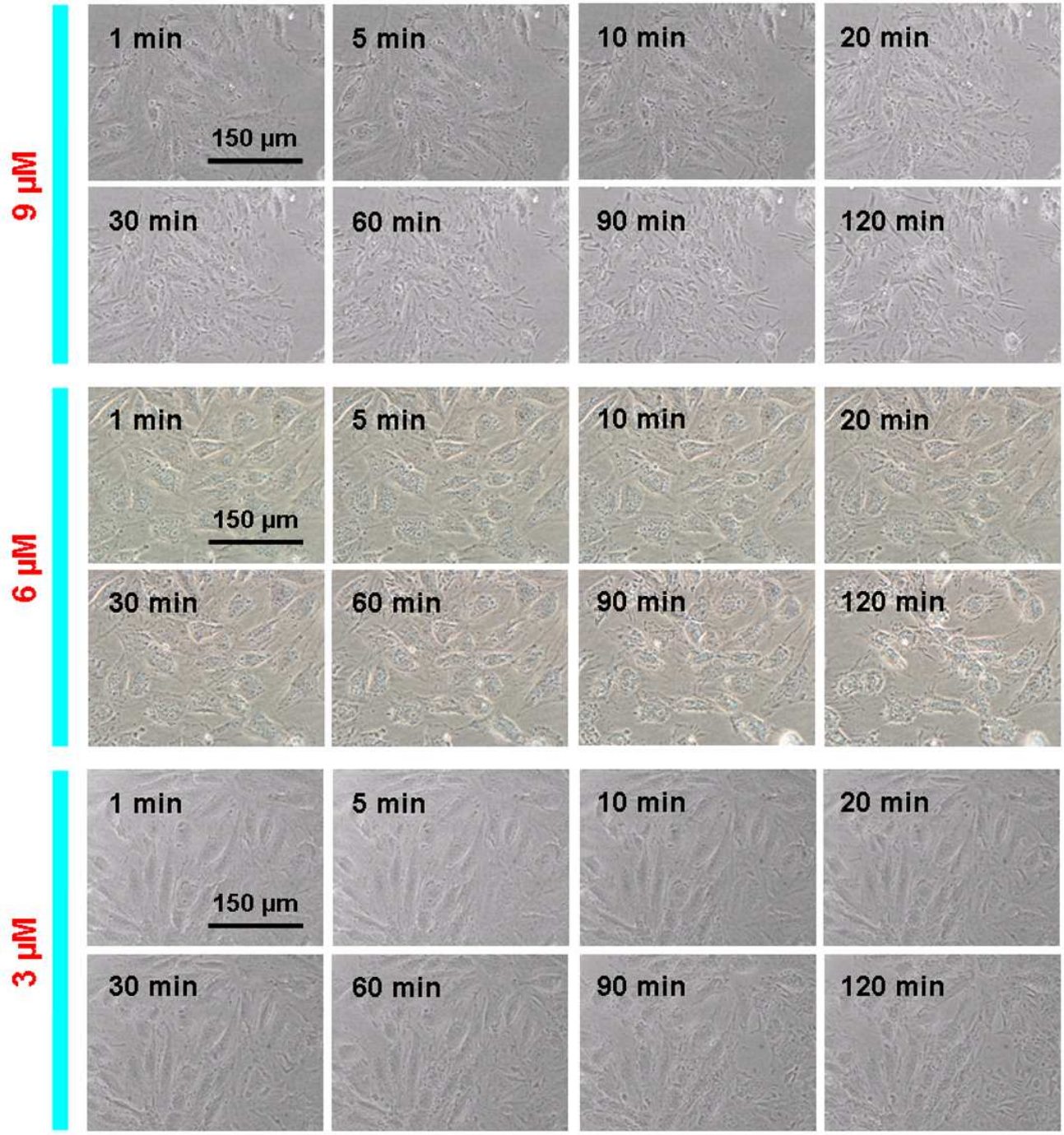

Figure S12. Morphological changes in the myocardial cells during FCCP hypoxia treatment at a concentration of 3, 6, and 9 μM using the conventional plate-based culture method.

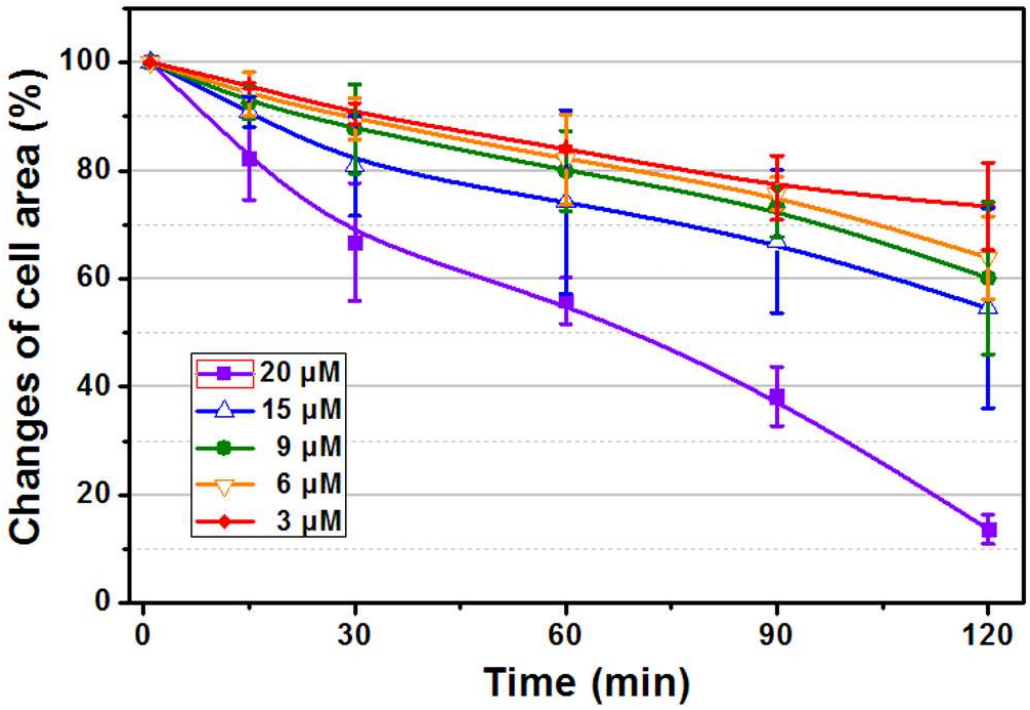

Figure S13. Changes in myocardial cell size during FCCP hypoxia treatment at various concentrations (i.e., 3, 6, 9, 15, and 20 μM) and at different treating times (i.e., 1, 15, 30, 60, 90, or 120 min) using the conventional plate-based culture method.

REFERENCES

(1) Li, L.; Ren, L., Liu, W.; Wang, J.-C.; Wang, Y.; Tu, Q.; Xu, J.; Liu, R.; Zhang, Y.; Yuan, M.-S.; Li, T.; Wang, J. *Anal. Chem.* **2012**, *84*, 6444–6453.

(2) Hung, P. J.; Lee, P J.; Sabounchi, P.; Lin, R.; Lee, L. P. *Biotechnol. Bioeng.* **2005**, *89*, 1–8.

(3) Taylor, A. M.; Blurton-Jones, M.; Rhee, S. W.; Cribbs, D. H.; Cotman, C. W.; Jeon, N. L. *Nat. Methods* **2005**, *2*, 599–605.

(4) Unekawa, M,; Tomita, M,; Tomita, Y,; Toriumi, H,; Miyaki, K,; Suzuki, N. *Brain Res.* **2010**, *1320*, 69–73.